Optimization of a Dedicated High Frequency Power Transformer for an Isolated 10kW Battery Charger for Industrial Use, by means of Electromagnetical Simulation

G. Pepato and M. Zignol
info@sirio-ic.com www.sirio-ic.com
Sirio Elettronica Srl - Via Selve, 2 I-35037 Bresseo di Teolo (PD) - Italy

ABSTRACT - In high frequency converters for industrial use, the efficiency is one of the most important feature to consider. In case of isolated converters, power transformer's losses are typically the distinguishing element while choosing the final solution. This paper analyzes the minimization of transformer's power losses, by evaluating the results of the electromagnetical simulations with different internal constructions.

Index terms: **Electromagnetical Simulation, Transformer, Eddy Losses, Skin Effect, Proximity Effect, Efficiency.**

I. Introduction

Several studies have been performed about the distribution of high frequency currents inside conducting materials. In fact, skin and proximity effects affect so much the efficiency of high frequency components, that they cannot be neglected. For power electronics developers, especially in case of inductive components, this knowledge is basic to design a high-efficiency solution.

This project has been studied by Sirio R&D team during the development of the high frequency power transformer dedicated to a 10 kW battery charger for industrial use. As we received this enquiry from one of our customers, this research is oriented by nature to the volume production. So, even if the real optimization of the transformer takes into account different aspects, such as losses, safety requirements and reliability, feasibility with available facilities and available raw materials, overall dimensions, and obviously price, this paper will focus on the losses minimization, by considering all other features as a background, only.

A. Aim of the work

The aim of this work is to compare losses of different internal constructions of the transformer by means of 2D electromagnetical simulation [22], performed by using ANSYS sofware, a finite element analysis (FEA) code widely used in the computer-aided engineering (CAE) field; to see the benefits coming from different ways of windings interleaving; to understand the right choice of different copper thickness. The design procedure and the electromagnetical model of the transformer will be briefly illustrated in the following paragraphs.

B. Literary background

The work of optimization of the design start from a solid literature background. As the main goal is the estimation of losses and efficiency, some references are useful to understand what is behind the figures. Generally, transformer losses are divided into Core Losses and Winding Losses.

Core Losses

Core Losses P_C are calculated from the specific losses given by the supplier of magnetic materials at various frequencies and flux densities. One of the most used estimation of core losses is based on the Steinmetz Equation [1], [2]:

$$P_C = C_m \cdot f^{\alpha} \cdot B_{max}^{\beta} \qquad (1)$$

and its implementations for non-sinusoidal fields [3], [5], [6], [7].

Winding Losses

When high frequency currents flow through conductors skin and proximity effects [9], [10], [11], [12], [14], [15], [19] have a high impact on losses, so Winding Losses P_W are not made by Joule Losses only.

Joule Losses

When DC windings resistance R_{DC} and rms currents I_{rms} through each winding (W_i) are known, Joule Losses P_J can be calculated from the contribution of each winding:

$$P_J = \Sigma_i (R_{DCWi} \cdot I_{rmsWi}^2) = \Sigma_i P_{JWi} = P_{JP} + P_{JS} \qquad (2)$$

Skin effect

The AC current density J in a conductor decreases exponentially from its value at the surface J_S according to the depth d from the surface, as follows:

$$J = J_S \cdot e^{-d/\delta} \qquad (3)$$

where δ is called the skin depth. The skin depth is thus defined as the depth below the surface of the conductor at which the current density has fallen to 1/e of J_S. In normal cases it is well approximated as:

$$\delta^2 = [(2 \cdot \rho)/(\omega \cdot \mu)] \qquad (4)$$

where ρ is the resistivity of the conductor, ω is the angular frequency of current, μ is the absolute magnetic permeability of the conductor.

Proximity effect

In a conductor carrying alternating current, if currents are flowing through one or more other nearby conductors the distribution of current within the first conductor will be constrained to smaller regions. The resulting current crowding is termed the proximity effect. This crowding gives an increase in the effective resistance of the circuit, which increases with frequency.

Skin Factor

The contribution of skin and proximity effects is taken into account by the skin factor f_R. If we refer to a single winding it is possible to specify the quantity $R_{AC} = f_R \cdot R_{DC}$.

Winding Losses can be calculated as:

$$P_{WP} + P_{WS} = P_W =$$
$$\Sigma_i (R_{ACWi} \cdot I_{rmsWi}^2) = \Sigma_i (f_R \cdot R_{DCWi} \cdot I_{rmsWi}^2) = \quad (5)$$
$$F_R \cdot \Sigma_i (R_{DCWi} \cdot I_{rmsWi}^2) = F_R \cdot P_J$$

Where F_R is the average contribution of the overall skin and proximity effects.

A winding solution is typically considered acceptable when Winding Losses are 50÷70% higher than Joule Losses.

The F_R ratio is strictly connected to the construction of the transformer and depends on the working frequency. To minimize F_R some strategies have to be used: to reduce the skin effect, thin conductors (thinner than the skin depth) have to be used (see litz wire [13], [16], [18] and copper foil); to reduce the proximity effect, good coupling and balanced position of windings is needed.

Total Losses

Total Losses P_T are defined as:

$$P_T = P_C + P_W = P_C + F_R \cdot P_J \quad (6)$$

so the efficiency can be expressed as:

$$\eta = P_{OUT} / (P_{OUT} + P_T) \quad (7)$$

C. Technical background

The technical background of this project comes from the 40 years Sirio's experience in the development and production of high frequency inductive components for industrial applications. All projects take advantage of the available technologies and production facilities, and especially two technologies are strictly connected to the final design and are responsable for the feasibility of the transformer. The most important one is the vacuum casting process, that allows to reach high isolation voltage in very thin distances. The control of the stability of the winding process through automation is fundamental as well to get the exact construction of the component, according to the drawing, and the costancy of features during volume production.

II. Design of the transformer

The design of the transformer is a process performed by trial and errors.

a. The project typically starts by choosing the most suitable magnetic material for the application; in case of high frequency inductive components, the magnetic material is chosen by looking mainly at the temperature range specification and the switching frequency. From the choice of the magnetic material come the maximum flux density and the optimum working ΔB range.

b. When the material is fixed, the second step is the definition of the size, that means the mechanical dimensions of the magnetic core and the available space for windings and isolating material. Some discrete mechanical parameters are useful to define a simple model and to proceed with the next two steps. The most important ones are minimum (l_{min}), average (l_{med}) and maximum (l_{max}) turn's length; depth (d_W), length (h_W) and width (w_W) of the winding volume; core's section (A_e) and volume (V_e), average magnetic path (l_e).

c. The third step is the calculation of the number of primary and secondary turns (N_P and N_S), according to the magnetic core's features, in terms of saturation and specific losses and in order to fulfil the input/output voltage ratio.

d. The fourth step is the formulation of several hypotesis concerning the construction of the transformer: primary winding section, secondary windings section, thickness of isolation, type of windings disposition and internal interconnection (series and parallel, when interleaving is considered). All solutions have to be reasonable, that means based on simmetry criteria and considering the skin depth, while choosing the conductors. A rough calculation of losses can be performed starting from the mechanical parameters (see step b.) and the converter's characteristics.

e. If either the first approximate evaluation or the simulation gives positive results, then it is worthwhile to perform some electromagnetical simulations to classify the solutions, regarding to the level of losses. If there is not any solution able to fulfil the efficiency specification, then it's needed to come back and start again from the step b. and change the size of the design.

III. Model of the transformer

Even if the level of approximation is higher and the right compromises have to be found, the 2D analysis [22] has been preferred to the 3D because it is much quicker in calculation and easiest in drawing. In effect, while the 3D model needs a 3D drawing, for the 2D version the section and some additional information about the complete design are enough. The whole design process of high frequency power transformers has been validated by many real applications, where the theoretical highest-efficiency solution corrisponded to the real highest-efficiency solution, even if the real value of transformer's losses was not possible to measure. It is, anyway, continuosly improving, to get faster and more accurate results.

The model is made of two parts: the physical model and the electrical model, that communicates through a bi-directional flow of information, to calculate the requested characteristics.

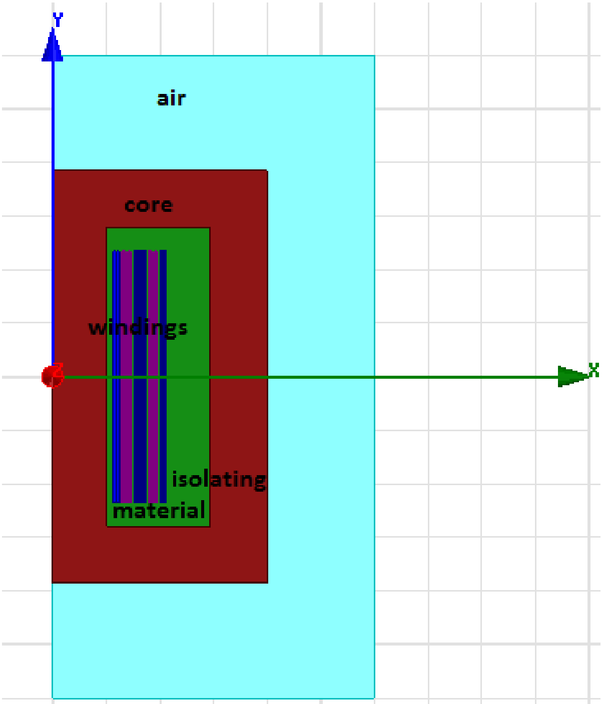

Figure 1 – Physical Model

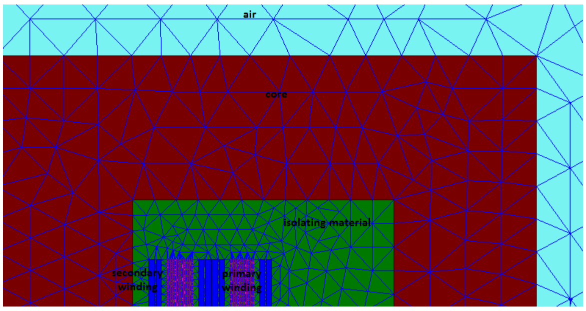

Figure 2 – Example of materials' particles mesh

Physical Model

The transformer is "cut" along a vertical section, where the core is involved (Figure 1). The analyzed area has to include some space around the core to define the boundary conditions. Inside the model area, several objects are identified: windings, core, air, isolating material. All objects are divided in small particles, creating a sort of mesh (Figure 2), where the software calculates electromagnetic fields and current distribution, solving Maxwell's equations. The model's simmetry and its depth have to be specified, to get the final results. This model gives information about fields, currents distribution, losses, ... on time and space domain. The figure shows how simmetry helps in calculation, in fact by solving just half the section we get the results of the whole section, that means the software takes half time to solve equations.

Electrical Model

The converter is represented by an electrical circuit, which provides data about the excitation conditions to the physical model. The transformer is made of coupled coils. This model give information about overall currents, voltages, powers, on time domain, only.

IV. The project

The transformer under consideration works in a Phase-Shifted Full-Bridge converter, with center tapped secondary winding.

Here below are the main characteristics:

- Input DC Voltage Range, V_{IN} = 550 ÷ 750 V
- DC Output Voltage, V_{OUT} = 44 V
- DC Output Current, I_{OUT} = 220 A
- Output Power, P_{OUT} = 9680 W
- Rated Switching Frequency, f_n = 53 kHz
- Temperature Range: -25°C ÷ +50°C
- P/S_1+S_2+case Isolation rms Voltage Test: 5 kVrms @ 50 Hz, 1'
- P:S turns ratio: $n = N_P/N_{S1} = N_P/N_{S2}$ = 10,5
- Output Ripple Current: ΔIpkpk = 20%Iout
- Transformer's Efficiency > 99,5%

Minimum input voltage is considered to perform simulations.

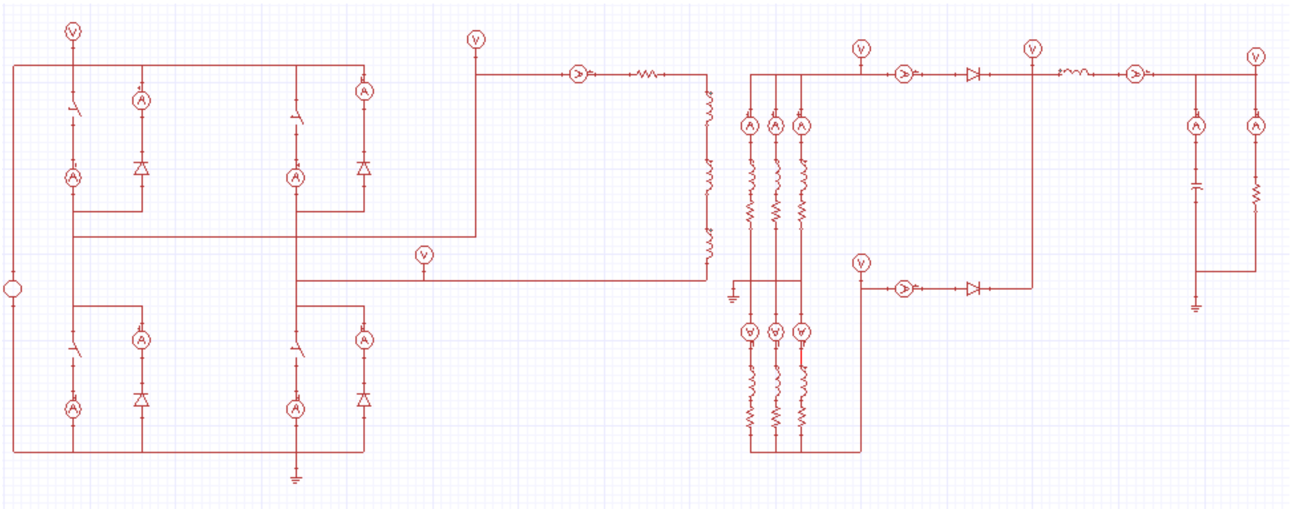

Figure 3 – Electrical Model

A. The magnetic material

The most suitable material for the specified switching frequency and the temperature range is MnZn ferrite material.

On the market N87 from EPC-TDK is available, suitable for power applications. The main limitations coming from this choice are the following:

$$B_{max} < 300 \text{ mT}$$

$$\Delta B_{50kHz\ opt} = 100 \div 260 \text{ mT}$$

B. The size

From theoretical point of view, transformer's dimensions are related mainly to two parameters: the switching frequency and the rated power. An easy formula says that the transformer's volume *VOL* is directly proportional to the Power(*P*) above Frequency(*f*) ratio:

$$VOL \propto P/f \qquad (8)$$

but that is just a quick way to make a first choice and to understand the approximate dimensions. The graphic shown in Figure 4 is a good overview about the Power/Frequency ratio, referred to Sirio's bobbin and boxes and based on multiple standard ferrite cores. It was extrapolated by looking at the results of several running projects, developed in the last years.

The P/f graphic suggests to use the 2xEE80 size (Figure 5), that means two pairs of EE80 cores.

Information from supplier of magnetic material side are reported here below (Figure 4).

Magnetic characteristics (per set)

$\Sigma l/A$ = 0.47 mm^{-1}
l_e = 184 mm
A_e = 390 mm^2
A_{min} = 388 mm^2
V_e = 71800 mm^3

Approx. weight 358 g/set

Ungapped

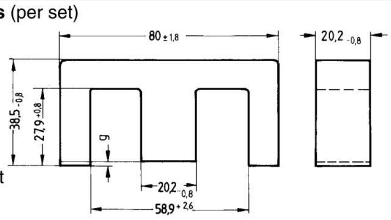

Material	A_L value nH	μ_e	P_V W/set
N87	4500 +30/–20%	1680	< 6.50 (100 mT, 100 kHz, 100 °C)

Figure4 – Magnetic characteristics of EE80 core

C. Number of turns and isolation thickness

By considering the optimum ΔB range, the number of secondary turns cannot be lower than 2. This is also the optimum value because, to minimize winding losses, the minimum number of secondary turns has to be considered. For all building solutions of this size, the turns ratio 21:2+2 and the F_R factor of 1,6 is considered for preliminary calculation.

Moreover, all construction ways are based on concentric windings made of copper foil, with isolated turns. Isolation requirements fulfil the safety standards requested by the customer so, inside the transformer, minimum distances through isolation are designed accordingly.

Currents can be calculated by standard formula of phase-shifted switching converters [8], getting:

$I_{Prmsth} = 19{,}50\ A$; $I_{S1rmsth} = I_{S2rmsth} = I_{Srmsth} = 150{,}30\ A$.

Figure 5 – Transformer based on 2 pairs of EE80 cores

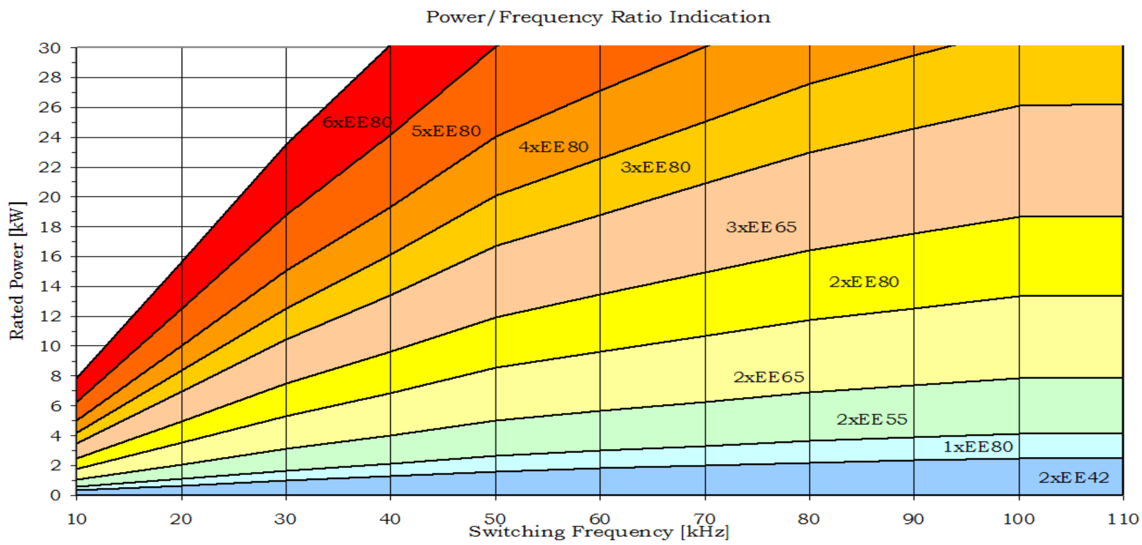

Figure 6 – Graphic for the choice of the size

D. Building solutions

In the table T1, all evaluated solutions are shown.

Due to the low input current (high voltage at the primary side) primary winding was split in *p* parts (*p* = 1, 2, 3; $\Sigma_{i=1}^{p} N_{Pi} = N_P$).

Because of the high output current (low voltage at the secondary side), *s* parallels were considered for each secondary winding (*s* = 1, 2, 3); secondary windings are divided in two groups: the *odd group* S1, S3, S5, connected in parallel and the *even group* S2, S4, S6, connected in parallel. All secondary windings are made of N_S turns ($N_{S1} = N_{S2} = N_{S3} = N_{S4} = N_{S5} = N_{S6} = N_S$).

Winding sequences were fixed and classified as following (the sequence starts from the inside of the bobbin and goes to the outside). All variations due to copper thickness are marked by subscrits.

solution zero:

$[N_{S1}]:[N_P]:[N_{S2}]$

solution A:

$[N_{S1}]:[(N_P+1)/2]: [N_{S2}]:[N_{S3}]:[(N_P-1)/2]:[N_{S4}]$

solution B:

$[N_P/3]:[N_{S1}]:[N_{S2}]:[N_P/3]:[N_{S3}]:[N_{S4}]:[N_P/3]$

solution C:

$[N_{S1}]:[N_P/3]:[N_{S2}]:[N_{S3}]:[N_P/3]:[N_{S4}]:[N_{S5}]:[N_P/3]:[N_{S6}]$

solution D:

$[(N_P-1)/4]:[N_{S1}]:[N_{S2}]:[(N_P+1)/2]:[N_{S3}]:[N_{S4}]:[(N_P-1)/4]$

solution E:

$[N_{S1}]:[(N_P-1)/4]:[N_{S2}]:[N_{S3}]:[(N_P+1)/2]:[N_{S4}]:[N_{S5}]:[(N_P-1)/4]:[N_{S6}]$

Copper thickness available: 0,08 – 0,16 – 0,20 – 0,30 – 0,40 – 0,50 mm; thicker thickness will be not considered because bigger than 2·δ.

		zero0	zero1	zero2	zero3	zero4	A0	A1	B0	B1	C0	C1	D0	D1	E0
th_P	[mm]	0,08	0,08	0,20	0,20	0,16	0,08	0,08	0,16	0,08	0,08	0,08	0,16	0,08	0,08
p		1	1	1	1	1	1	1	1	1	1	1	1	1	1
th_S	[mm]	0,50	0,40	0,50	0,40	0,40	0,50	0,40	0,40	0,40	0,30	0,40	0,40	0,40	0,30
s		1	1	1	1	1	2	2	2	2	3	3	2	2	3
N_{P1}	Turns	21	21	21	21	21	11	11	7	7	7	7	5	5	5
N_{P2}	Turns						10	10	7	7	7	7	11	11	11
N_{P3}	Turns								7	7	7	7	5	5	5
N_{S1}	Turns	2	2	2	2	2	2	2	2	2	2	2	2	2	2
N_{S2}	Turns	2	2	2	2	2	2	2	2	2	2	2	2	2	2
N_{S3}	Turns						2	2	2	2	2	2	2	2	2
N_{S4}	Turns						2	2	2	2	2	2	2	2	2
N_{S5}	Turns										2	2			2
N_{S6}	Turns										2	2			2
R_{DCP1th}	[mohm]	18,10	17,90	7,60	7,56	9,29	9,12	9,03	2,69	5,31	5,61	5,66	2,02	3,76	4,01
R_{DCP2th}	[mohm]						10,12	9,90	3,27	6,33	6,52	6,67	5,46	9,94	10,49
R_{DCP3th}	[mohm]								3,85	7,34	7,43	7,69	2,94	5,28	5,53
R_{DCS1th}	[mohm]	0,24	0,30	0,24	0,30	0,30	0,24	0,30	0,33	0,33	0,40	0,30	0,33	0,32	0,30
R_{DCS2th}	[mohm]	0,31	0,38	0,34	0,42	0,41	0,29	0,36	0,35	0,34	0,45	0,34	0,34	0,33	0,34
R_{DCS3th}	[mohm]						0,30	0,37	0,40	0,38	0,47	0,36	0,41	0,39	0,35
R_{DCS4th}	[mohm]						0,35	0,42	0,41	0,40	0,52	0,40	0,42	0,40	0,41
R_{DCS5th}	[mohm]										0,54	0,42			0,42
R_{DCS6th}	[mohm]										0,59	0,46			0,46
I_{Prmsth}	[A]	19,50	19,50	19,50	19,50	19,50	19,50	19,50	19,50	19,50	19,50	19,50	19,50	19,50	19,50
I_{Srmsth}	[A]	150,30	150,30	150,30	150,30	150,30	150,30	150,30	150,30	150,30	150,30	150,30	150,30	150,30	150,30
P_{JPth}	[W]	6,88	6,81	2,89	2,87	3,53	7,32	7,20	3,73	7,22	7,44	7,61	3,96	7,22	7,61
P_{JSth}	[W]	12,42	15,36	13,10	16,26	16,04	6,59	8,12	8,35	8,11	7,35	7,85	8,37	14,78	14,48
P_{Jth}	[W]	19,31	22,17	15,99	19,14	19,57	13,91	15,32	12,08	15,33	14,79	15,46	12,34	22,00	22,10
P_{Cth}	[W]	7,06	7,06	7,06	7,06	7,06	7,06	7,06	7,06	7,06	7,06	7,06	7,06	7,06	7,06
P_{Tth}	[W]	37,95	42,53	32,65	37,68	38,37	29,32	31,57	26,39	31,59	30,73	31,80	26,80	42,26	42,42
η_{th}	[%]	99,61	99,56	99,66	99,61	99,61	99,70	99,67	99,73	99,67	99,68	99,67	99,72	99,57	99,56

Meaning of variables: th_P primary thickness; th_S secondary thickness; *p* number of primary parallel connections; *s* number of each secondary parallel connections; N_{Pi}, N_{Si} number of turns (P primary, S secondary); R_{DCPith} theoretical winding's DC resistance values of the i^{th} primary winding; R_{DCSith} theoretical winding's DC resistance values of the i^{th} secondary winding; I_{Prmsth} theoretical rms primary current; I_{Srmsth} theoretical rms secondary current; P_{JPth} theoretical primary joule losses; P_{JSth} theoretical secondary joule losses (both secondary windings); P_{JPth} theoretical joule losses; P_{Cth} theoretical core losses; P_{Tth} theoretical total losses (case of F_R=1,6); η_{th} theoretical efficiency.

Table 1 – Analisys of possible solution before simulation

V. Analisys of results

		zero0	zero1	zero2	zero3	zero4	A0	A1	B0	B1	C0	C1	D0	D1	E0
th_P	[mm]	0,08	0,08	0,20	0,20	0,16	0,08	0,08	0,16	0,08	0,08	0,08	0,16	0,08	0,08
p		1	1	1	1	1	1	1	1	1	1	1	1	1	1
th_S	[mm]	0,50	0,40	0,50	0,40	0,40	0,50	0,40	0,40	0,40	0,30	0,40	0,40	0,40	0,3
s		1	1	1	1	1	2	2	2	2	3	3	2	2	3
N_{P1}	Turns	21	21	21	21	21	11	11	7	7	7	7	5	5	5
N_{P2}	Turns						10	10	7	7	7	7	11	11	11
N_{P3}	Turns								7	7	7	7	5	5	5
N_{S1}	Turns	2	2	2	2	2	2	2	2	2	2	2	2	2	2
N_{S2}	Turns	2	2	2	2	2	2	2	2	2	2	2	2	2	2
N_{S3}	Turns						2	2	2	2	2	2	2	2	2
N_{S4}	Turns						2	2	2	2	2	2	2	2	2
N_{S5}	Turns										2	2			2
N_{S6}	Turns										2	2			2
I_{OUT}	[A]	219,10	219,02	218,82	218,73	218,91	220,07	220,09	219,98	219,97	220,29	220,32	220,09	220,06	220,57
I_{P1rms}	[A]	20,75	20,75	20,80	20,79	20,79	20,60	20,60	20,74	20,64	20,40	20,42	20,71	20,59	20,52
I_{P2rms}	[A]						20,60	20,60	20,74	20,64	20,40	20,42	20,71	20,59	20,52
I_{P3rms}	[A]								20,74	20,64	20,40	20,42	20,71	20,59	20,52
I_{S1rms}	[A]	154,48	154,44	154,57	154,50	154,53	80,08	80,56	93,45	92,73	52,92	52,09	77,89	77,40	46,16
I_{S2rms}	[A]	154,46	154,40	154,54	154,45	154,55	80,02	80,34	69,49	69,23	55,29	57,04	82,99	82,47	51,84
I_{S3rms}	[A]						74,21	73,74	63,65	64,21	50,88	50,80	77,05	77,09	66,38
I_{S4rms}	[A]						71,31	71,97	89,24	89,20	50,73	50,38	71,71	71,79	66,25
I_{S5rms}	[A]										49,89	50,84			45,78
I_{S6rms}	[A]										47,86	46,78			40,21
P_{JP}	[W]	7,79	7,71	3,29	3,27	4,02	8,16	8,03	4,22	8,09	8,14	8,35	4,47	8,05	8,43
P_{JS}	[W]	13,12	16,21	13,85	17,18	16,96	6,83	8,40	9,46	9,17	7,75	5,96	8,94	8,58	6,54
P_J	[W]	20,92	23,92	17,14	20,45	20,97	14,99	16,44	13,68	17,26	15,89	14,30	13,41	16,63	14,97
P_{OUT}	[W]	9600,6	9593,7	9576,3	9568,8	9584,0	9686,1	9686,1	9678,4	9677,1	9705,4	9707,8	9688,2	9685,6	9730,3
P_C	[W]	7,71	7,72	7,71	7,71	7,72	7,82	7,82	7,87	7,85	7,84	7,85	7,86	7,84	7,83
P_{WP1}	[W]	18,15	17,90	54,26	53,73	39,95	5,17	5,12	5,48	3,48	2,62	2,66	2,51	2,02	1,80
P_{WP2}	[W]						5,49	5,37	2,77	3,05	5,56	3,14	7,77	5,59	5,79
P_{WP3}	[W]								7,72	4,73	3,47	3,62	3,59	2,82	2,48
P_{WS1}	[W]	18,32	16,88	18,40	17,08	17,04	4,88	4,88	7,37	7,11	1,74	1,78	4,41	4,17	0,89
P_{WS2}	[W]	23,43	21,23	25,69	23,61	23,02	6,02	5,98	3,16	2,98	2,10	2,21	5,32	5,12	1,29
P_{WS3}	[W]						5,16	5,09	3,29	3,13	1,95	2,08	6,00	5,58	2,94
P_{WS4}	[W]						5,76	5,53	8,84	8,43	2,16	2,31	5,24	4,92	3,39
P_{WS5}	[W]										2,19	2,44			1,33
P_{WS6}	[W]										2,27	2,48			1,12
P_{WP}	[W]	18,15	17,90	54,26	53,73	39,95	10,66	10,49	15,98	11,26	11,64	9,42	13,87	10,43	10,06
P_{WS}	[W]	41,75	38,11	44,10	40,69	40,06	21,81	21,47	22,66	21,65	12,40	13,29	20,98	19,80	10,95
P_W	[W]	59,89	56,01	98,36	94,42	80,01	32,47	31,96	38,64	32,91	24,04	22,71	34,85	30,23	21,01
F_R		2,86	2,34	5,74	4,62	3,82	2,17	1,94	2,82	1,91	1,51	1,59	2,60	1,82	1,40
P_T	[W]	67,60	63,73	106,07	102,13	87,73	40,29	39,78	46,51	40,76	31,88	30,56	42,71	38,07	28,84
η	[%]	99,30	99,34	98,90	98,94	99,09	99,59	99,59	99,52	99,58	99,67	99,69	99,56	99,61	99,70

Meaning of variables: th_P primary thickness; th_S secondary thickness; n_P number of primary parallel connections; n_S number of each secondary parallel connections; N_{Pi}, N_{Si} number of turns (P primary, S secondary); I_{OUT} output current (Electrical Simulation, EL); $I_{Pirmsth}$ rms current through a single primary (EL); $I_{Sirmsth}$ rms current through a single secondary (EL); P_{JP} primary joule losses (EL); P_{JS} secondary joule losses (EL); P_{JP} total joule losses; P_{OUT} output power (EL); P_C core losses (Electromagnetical Simulation EM); P_{WPi} winding losses of a single primary (EM); P_{WSi} winding losses of a single secondary (EM); P_{WP} primary winding losses (EM); P_{WS} secondary winding losses (EM); P_W total winding losses (EM); F_R skin factor; η efficiency.

Table 1 – Results of simulation

All simulated solutions converge to the same steady-state values of voltage, current, power. In the figures below some examples are shown for reference.

The table 2 is the sum-up of simulations. All values are the rms values in the same period.

Core losses are not substantially modified by the internal construction of the transformer, as it was deduced from theoretical calculation.

By looking at the "zero" building solutions, it is evident that a copper thickness increase doesn't lead to a decrease of winding losses: this means that while joule losses decrease, the parasitic losses increases much more. The F_R factor reaches the maximum value with the thickest thickness and the minimum value with the thinnest thickness. Even if theoretical efficiency values of the studied solutions were all higher than 99,5%, we found that zero version doesn't fulfil the efficiency requirement.

As the complexity of internal structure increases the coupling between windings improves due to the lower number of primary layers in each portion and to the wider mating surface. Moreover as we have already seen in the zero case, by reducing thickness of windings, the F_R ratio can be further reduced.

More sophysticated solutions have to be developed according to simmetry criteria. Three interesting comparisons can be perfomed between solutions B0 and D0, solutions B1 and D1, solutions C0 and E0, where only the primary partition changes. For all three cases, the solution built with 11 turns in the central primary portion is more efficient. The reason is the perfectly symmetrical coupling.

Presently, theoretical thermal considerations are made by taking into account the thermal resistance of materials. Due to the mix of different materials and the complexity of the boundary conditions (components layout, cooling system, environment and so on), it is not possible to predict exact figures about the changing of the temperature with the efficiency. As a result, the most precise evaluation of overtemperature and steady-state temperature is available by measurement with probes on the application. It could be an interesting study for the future to create a model that integrates thermal features in the design.

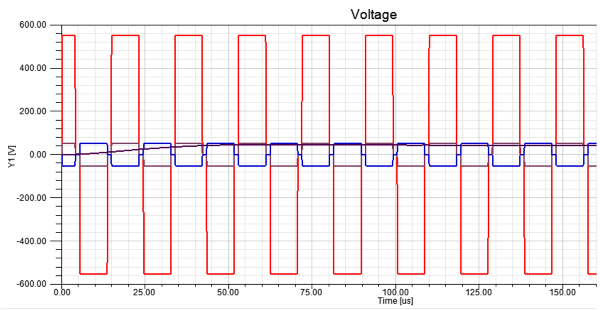

Figure 7 – Primary, secondary and output voltage

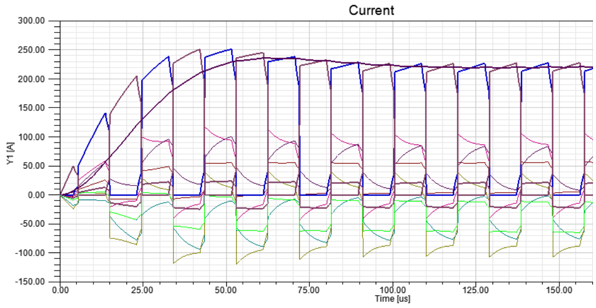

Figure 8 – Current through windings and output current

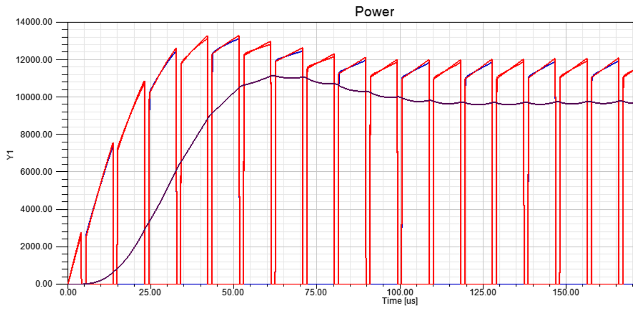

Figure 9 – Input and output power

Figure 10 – Core and Joule Losses

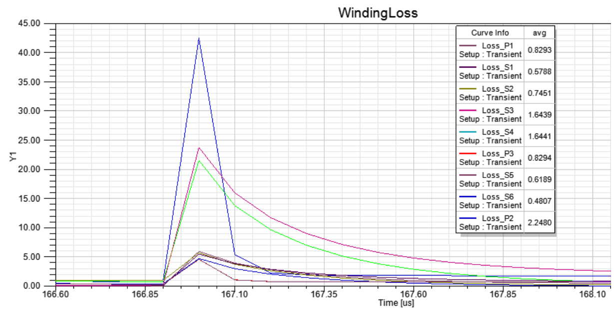

Figure 10 – Winding Losses

The curious thing of this project is that, due to the cost of a solution complicated by a too sophysticated winding process, the customer did not choose the most efficient solution.

References

[1] C.P. Steinmetz, "On the Law of Hysteresis," AIEE Transactions, vol. 9, pp. 3-64, 1892, Reprinted under the title "A Steinmetz Contribution to the Ac Power Revolution", introduction by J. E. Brittain, in Proceedings of the IEEE, vol. 72(2), pp. 196-221, Feb. 1984.

[2] E.C. Snelling, "Soft Ferrites, Properties and Applications", Butterworths, second edition, London (UK), 1988.

[3] L.H. Dixon, "Magnetics Design for Switching Power Supplies – Magnetic Core Characteristics".

[4] L.H. Dixon, "Magnetic Core Properties" (R1), originally titled "An Electrical Circuit Model for Magnetic Cores", Unitrode Seminar Manual SEM1OOO, 1995.

[5] J. Li, T. Abdallah and C.R. Sullivan, "Improved Calculation of Core Loss with Nonsinusoidal Waveforms," in Proceedings of 36th Annual Meeting of the IEEE Industry Applications Society, vol. 4, pp. 2203-2210, 2001.

[6] K. Venkatachalam, C.R. Sullivan, T. Abdallah and H. Tacca, "Accurate Prediction of Ferrite Core Loss with Nonsinusoidal Waveforms Using Only Steinmetz Parameters", Compel 2002: 8th IEEE Workshop On Computers In Power Electronics.

[7] D. Lin, P. Zhou, W.N. Fu, Z. Badics and Z.J. Cendes, "A Dynamic Core Loss Model for Soft Ferromagnetic and Power Ferrite Materials in Transient Finite Element Analysis", Compumag 2003.

[8] M. Sippola, "Developments for The High Frequency Power Transformer Design and Implementation", Jun. 2003.

[9] P.L. Dowell, "Effects of Eddy Currents in Transformer Windings", Proceeding of the IEEE (UK), vol. 113, no. 8, pp. 1387-1394, Aug. 1966.

[10] Lloyd H. Dixon, "Magnetics Design for Switching Power Supplies – Windings".

[11] Lloyd H. Dixon, "Eddy Current Losses in Transformer Windings and Circuit Wiring" (R2), Unitrode Seminar Manual SEM600, 1988.

[12] J.A. Ferreira, "Improved Analytical Modeling of Conductive Losses in Magnetic Components," IEEE Trans. Power Electron., vol. 9, pp. 127-131, Jan. 1994.

[13] C.R. Sullivan, "Optimal Choice for Number of Strands in a Litz-Wire Transformer Winding", IEEE Transactions on Power Electronics, vol. 14, no. 2, pp. 283-291, Mar. 1999.

[14] C.R. Sullivan, "Winding Loss Calculation with Multiple Windings, Arbitrary Waveforms and 2-D Field Geometry," in Proc. 1999 IEEE Ind. Applicat. Soc. Annu. Meeting, pp. 2093–2099, 1999.

[15] C.R. Sullivan, "Computationally Efficient Winding Loss Calculation with Multiple Windings, Arbitrary Waveforms, and Two-Dimensional or Three-Dimensional Field Geometry", IEEE Transactions on Power Electronics, vol. 16(1), no. 1, pp. 142–150, Jan. 2001.

[16] C.R. Sullivan, "Cost-Constrained Selection of Strand Wire and Number in a Litz-Wire Transformer Winding", IEEE Transactions On Power Electronics, vol. 16, no. 2, Mar. 2001.

[17] C.R. Sullivan, T. Abdallah and T. Fujiwara, "Optimization of a Flyback Transformer Winding Considering Two-Dimensional Field Effects, Cost and Loss", in Proceedings of 16th Annual Applied Power Electronics Conference - APEC 2001, vol. 1, pp. 116–22, 2001.

[18] J. Pollock, T. Abdallah, and C.R. Sullivan, "Easy-To-Use CAD Tools For Litz-Wire Winding Optimization", in Proceedings of 18th Annual Applied Power Electronics Conference - APEC 2003, 2003.

[19] X. Nan and C.R. Sullivan, "An Improved Calculation of Proximity-Effect Loss in High-Frequency Windings of Round Conductors", 34th Annual IEEE Power Electronics Specialists Conference, 2003.

[20] M. Albach, "Two-dimensional calculation of winding losses in transformers".

[21] F. Hoke and C.R. Sullivan, "An Improved Two-Dimensional Numerical Modeling Method for E-Core Transformers", in IEEE Applied Power Electronics Conference, vol. 1, pp. 151-7, 2002.

[22] S. Wang, "Modeling and Design of Planar Integrated Magnetic Components", Jul. 2003. Ansoft Corporation, Maxwell finite element analysis software, Pittsburgh, PA.